Selective binding of perfringolysin O derivative to cholesterol-rich membrane microdomains (rafts)

A. A. Waheed*†, Yukiko Shimada*, Harry F. G. Heijnen‡, Megumi Nakamura*, Mitsushi Inomata*, Masami Hayashi*, Shintaro Iwashita§, Jan W. Slot¶, and Yoshiko Ohno-Iwashita*†

*Department of Protein Biochemistry, Tokyo Metropolitan Institute of Gerontology, 35-2 Sakae-cho, Itabashi-ku, Tokyo 173-0015, Japan; ‡Department of Hematology, Division on Thrombosis and Hemostasis and ¶Department of Cell Biology and Institute for Biomembranes, University Medical Center Utrecht, 3508 GA Utrecht, The Netherlands; and §Mitsubishi Kasei Institute of Life Sciences, Machida, Tokyo 194-8511, Japan

Communicated by William T. Wickner, Dartmouth Medical School, Hanover, NH, February 23, 2001 (received for review December 4, 2000)

There is increasing evidence that sphingolipid- and cholesterol-rich microdomains (rafts) exist in the plasma membrane. Specific proteins assemble in these membrane domains and play a role in signal transduction and many other cellular events. Cholesterol depletion causes disassembly of the raft-associated proteins, suggesting an essential role of cholesterol in the structural maintenance and function of rafts. However, no tool has been available for the detection and monitoring of raft cholesterol in living cells. Here we show that a protease-nicked and biotinylated derivative (BCθ) of perfringolysin O (θ-toxin) binds selectively to cholesterol-rich microdomains of intact cells, the domains that fulfill the criteria of rafts. We fractionated the homogenates of nontreated and Triton X-100-treated platelets after incubation with BCθ on a sucrose gradient. BCθ was predominantly localized in the floating low-density fractions (FLDF) where cholesterol, sphingomyelin, and Src family kinases are enriched. Immunoelectron microscopy demonstrated that BCθ binds to a subpopulation of vesicles in FLDF. Depletion of 35% cholesterol from platelets with cyclodextrin, which accompanied 76% reduction in cholesterol from FLDF, almost completely abolished BCθ binding to FLDF. The staining patterns of BCθ and filipin in human epidermoid carcinoma A431 cells with and without cholesterol depletion suggest that BCθ binds to specific membrane domains on the cell surface, whereas filipin binding is indiscriminate to cell cholesterol. Furthermore, BCθ binding does not cause any damage to cell membranes, indicating that BCθ is a useful probe for the detection of membrane rafts in living cells.

Accumulating studies suggest that in eukaryotic cells membrane proteins are compartmentalized into dynamic microdomains [also known as rafts or detergent-resistant membranes (DRMs); refs. 1–6]. These domains are enriched in cholesterol and sphingolipids and contain glycosylphosphatidylinositol-anchored and acylated proteins (2, 3, 6–9). Cholesterol plays an important role in maintaining membrane rafts in a separate phase from the rest of the bilayer, a state similar to the liquid-ordered phase (l_o) described in model membranes (1–4, 10). Changes in cholesterol content affect the localization of proteins associated in rafts (9, 10), and thus affect the raft function. To understand the role of rafts in various cellular functions, identification and analysis of the molecular organization of cholesterol in rafts are essential. Cholesterol-binding toxin would be a useful tool for such a purpose (11).

θ-Toxin (perfringolysin O), a thiol-activated cytolysin produced by *Clostridium perfringens*, binds to membrane cholesterol (11–18), and then forms oligomeric pores causing membrane damage (18, 19). The C-terminal amino acid residues are essential for its activity (15, 18). The three-dimensional structure of θ-toxin has been shown recently (19). The digested θ-toxin with subtilisin Carlsberg protease (Cθ) is a complex of 38- and 15-KDa fragments and loses the capacity of oligomerization, resulting in no hemolytic activity below 20°C (12, 13). Biotinylated Cθ (BCθ) (11) has the same binding affinity to membrane cholesterol as wild-type θ-toxin and Cθ. BCθ possesses no

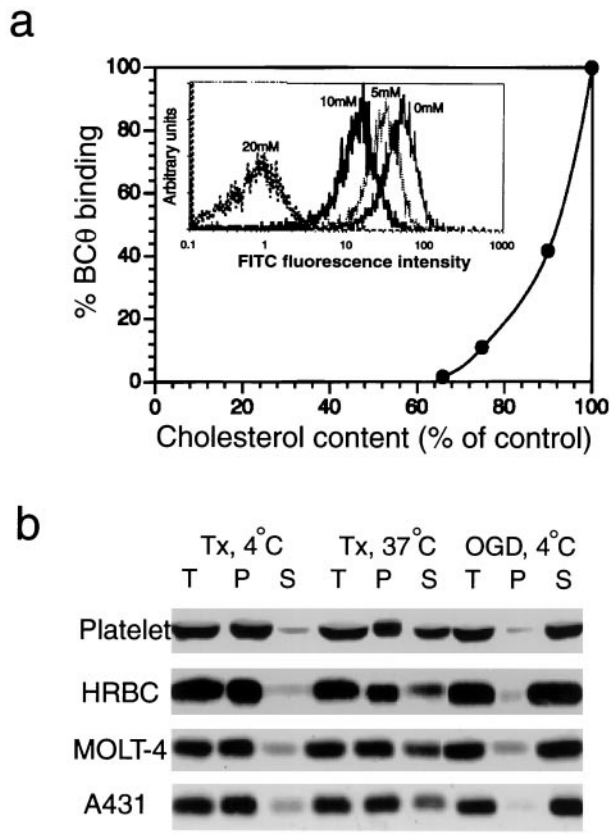

Fig. 1. Characteristics of BCθ binding to intact cells. (*a*) BCθ binding depends on cholesterol contents in cell membranes. Cholesterol was depleted from platelets with 5, 10, and 20 mM 2OHpβCD. The amount of BCθ bound to the platelets was quantified by flow-cytometric analysis (*Inset*) using fluorescein–avidin and plotted against cholesterol content. The values are expressed as percentage of nontreated control. Cholesterol in untreated platelets was 33 mol% of total lipids. (*b*) BCθ bound to cells was retained in the Tx-insoluble fraction. After incubation with BCθ, platelets, erythrocytes, MOLT-4, and A431 cells were extracted with 1% Tx (4°C or 37°C) or 60 mM octyl glucoside (OGD) (4°C) and the insoluble fraction was separated by centrifugation at 15,000 × *g*. The distribution of BCθ in insoluble pellet and soluble fractions were determined. T, total; P, pellet; S, soluble fractions.

Abbreviations: θ-toxin, perfringolysin O; Cθ, θ-toxin nicked with subtilisin Carlsberg protease; BCθ, biotinylated Cθ; Tx, Triton X-100; FLDF, floating low-density fractions; MβCD, methyl-β-cyclodextrin; 2OHpβCD, 2-hydroxypropyl-β-cyclodextrin; IEM, immunoelectron microscopy.

†To whom reprint requests may be addressed. E-mail: awaheed@tmig.or.jp or iwashita@tmig.or.jp.

The publication costs of this article were defrayed in part by page charge payment. This article must therefore be hereby marked "*advertisement*" in accordance with 18 U.S.C. §1734 solely to indicate this fact.

www.pnas.org/cgi/doi/10.1073/pnas.091090798

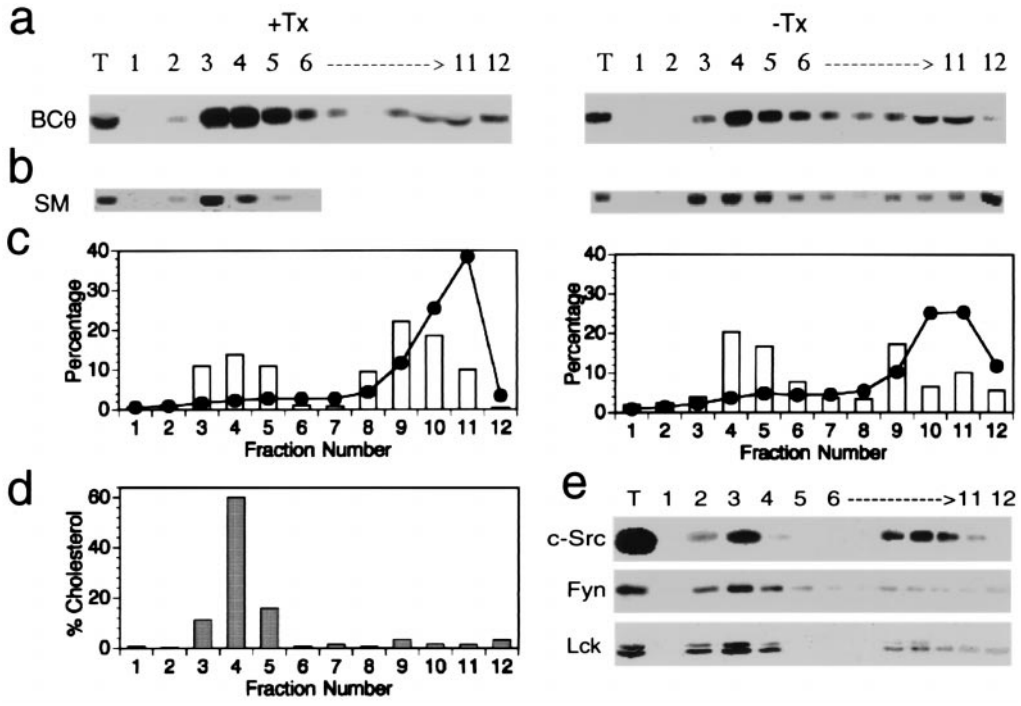

Fig. 2. BCθ is enriched in FLDF. BCθ-bound platelets were treated with (+Tx) or without Tx (-Tx), sonicated, subjected to a sucrose gradient centrifugation, and fractionated from the top (fractions 1–11 and pellet, fraction 12). The distribution of BCθ (*a*, +Tx and -Tx), cholesterol (*c*, open bars, +Tx and -Tx), and total protein (*c*, closed circles, +Tx and -Tx) in the gradient fractions was analyzed. In parallel experiments the distribution of sphingomyelin (SM) (*b*, +Tx and -Tx) and tyrosine-kinases (*e*, +Tx) was determined. (*d*) The Tx-insoluble pellet obtained at 4°C by centrifugation at 15,000 × *g* was subjected to density gradient fractionation and the cholesterol content in each fraction was determined. T, total platelets. On BCθ binding a shift in the distribution patterns of lipids and proteins was observed from fractions 2–4 to fractions 3–5 (+Tx). Because Tx in bottom fractions (7–12) interferes with the separation of lipids on TLC plates, the distribution pattern of sphingomyelin in these fractions was not shown (*b*, +Tx).

hemolytic activity even at 37 °C and has been used as a probe to evaluate the effects of cellular events on the topology and distribution of cholesterol (11, 16, 17). By using artificial membranes we have demonstrated that θ-toxin and its derivatives selectively bind to cholesterol in cholesterol-rich membranes (14, 20). Based on this we hypothesized that the θ-toxin and its derivatives could bind to cholesterol-rich microdomains of intact cells. In this report we characterized BCθ binding to intact cells biochemically and immunocytochemically and demonstrate selective binding of BCθ to cholesterol-rich microdomains (rafts) of intact cells. We also compared BCθ binding with known cholesterol binding probe filipin with and without cholesterol depletion in human A431 cells.

Materials and Methods

Materials. Anti-Lck, Anti-Lyn, and Anti-Fyn were purchased from Santa Cruz Biotechnology. Anti-c-Src was obtained from Upstate Biotechnology (Lake Placid, NY). Anti-θ-toxin antibody was prepared as described (15). Cyclodextrins were obtained from Sigma and filipin from Polysciences. A bicinchoninic acid protein assay kit was purchased from Pierce. Enhanced chemiluminescence (ECL) was procured from Amersham Pharmacia.

Preparation of θ-Toxin and Its Derivatives. θ-Toxin was overexpressed in *Escherichia coli* and purified from the periplasmic fractions as described (15). A nicked θ-toxin (Cθ) was obtained by using subtilisin Carlsberg digestion (12) and BCθ was prepared as described (11).

Cells and Cholesterol Depletion. Four different types of cells were used to check BCθ binding. Blood was collected from healthy volunteers who had not taken any drugs for 2 weeks. Platelets were isolated from fresh blood, anticoagulated with 0.1 volume of 3.8% tri-sodium citrate, and washed twice with Hepes–Tyrode's buffer (pH 6.7) supplemented with 0.5 units/ml apyrase and 0.35% BSA (21). The platelets were resuspended in Hepes–Tyrode's buffer (pH 7.4) at a concentration of 10^9 cells/ml. Human erythrocytes were washed four times with PBS (pH 7.4) before use. MOLT-4 cells established from T lymphocytes (22) and human epidermal carcinoma A431 cells (23) were maintained in DMEM supplemented with 10% FBS and washed with PBS before use. To deplete membrane cholesterol platelets were incubated with various concentrations of either methyl-β-cyclodextrin (MβCD) or 2-hydroxypropyl-β-cyclodextrin (2OHpβCD) in Hepes–Tyrode's buffer (pH 7.4) at 37°C for 30 min and washed twice with PBS.

BCθ Binding and Detergent Extraction. Cells were incubated with BCθ (5–10 μg/ml) in PBS containing 1 mg/ml BSA (the concentration of BCθ to cholesterol was kept constant in all four cell types) at 25°C for 20 min, and washed twice with the same volume of PBS to remove unbound BCθ. In some cases the amount of BCθ bound to intact cells were quantified by EPICS (Hialeah, FL) Elite flow cytometer after labeling with fluorescein–avidin as described (11).

After incubation with BCθ platelets, erythrocytes and MOLT-4 cells were brought to 4°C and then suspended in Mes-buffered saline (pH 6.5) containing detergent (1% Triton X-100, Tx, or 60 mM octyl glucoside), 10 mM EGTA and protease inhibitors. In the case of A431 cells, the cells were first scraped, suspended in Mes-buffered saline, spun down, and then treated with detergents as above. After incubating for 20 min at 4°C or 37°C the detergent-insoluble pellet was collected by centrifugation at 15,000 × *g* for 15 min.

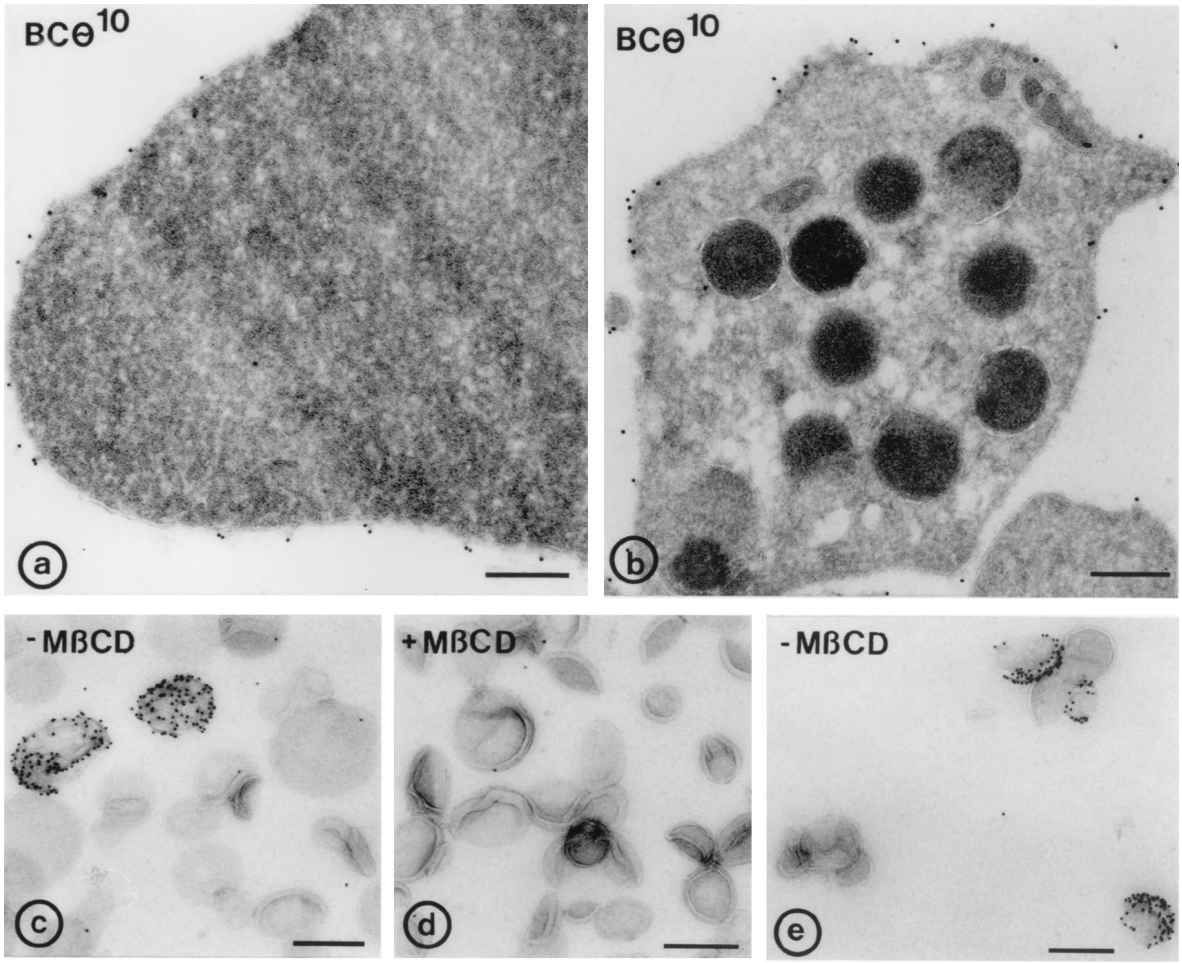

Fig. 3. IEM detection of cholesterol on erythrocytes, resting platelets, and isolated low-density membranes. (*a* and *b*) IEM detection of cell surface cholesterol of erythrocytes (*a*) and platelets (*b*). Washed cells were incubated with BCθ. Ultrathin cryosections were immunolabeled with anti-biotin and 10 nm protein-A gold. (*c* and *d*) Low-density membranes isolated from platelets by sucrose gradient centrifugation after BCθ binding. BCθ was immunolabeled with anti-biotin and 10 nm protein-A gold. High labeling is observed on a subpopulation of FLDF (*c*), and is completely abolished after depletion of membrane cholesterol with MβCD (*d*). (*e*) Low-density membranes were first isolated and then incubated with BCθ, followed by immunolabeling. A larger number of these membranes ($\approx$30%) bound the toxin as compared with the isolation after BCθ binding. (Bars: *a* and *b*, 200 nm; *c*–*e*, 250 nm.)

Sucrose Gradient Fractionation. After BCθ binding platelets were treated or untreated with Triton X-100 (Tx) and sonicated for 20 sec pulses (two and six times, respectively) by using a tip-type sonicator. Both homogenates were adjusted to 40% sucrose (wt/vol), overlaid with 2.4 ml of 36% sucrose and 1.2 ml of 5% sucrose in Mes-buffered saline (pH 6.5), centrifuged at 45,000 rpm (250,000 $\times$ *g*) for 18 h at 4°C in a SW55 rotor, and fractionated from the top (0.4 ml each, a total of 11 fractions). The pellet was suspended in 0.4 ml of Mes-buffered saline (pH 6.5), sonicated, and designated as 12th fraction. To aliquots of each fraction of the gradient SDS sample buffer containing 2-mercaptoethanol was added. The samples were stored at $-$20°C until use.

Biochemical Assays, PAGE, and Immunoblotting. Proteins in the gradient fractions were analyzed by using a bicinchoninic acid protein assay kit. Cholesterol was quantified enzymatically by using cholesterol oxidase (24). Lipids were extracted in chloroform/methanol and separated on TLC plates by using two solvent systems, and detected as described (11). Equal volumes of each gradient fraction were used for detecting distribution of BCθ, sphingomyelin, and cholesterol. BCθ was detected by immunoblotting using anti-θ-toxin antibody after SDS/PAGE. To detect raft-associated kinases in the gradient fractions, equal amounts of protein were loaded on 12% polyacrylamide gels and subjected to electrophoresis and immunoblotting.

Electron Microscopy. After BCθ binding, the platelets and erythrocytes were fixed in a mixture of 2% paraformaldehyde and 0.2% glutaraldehyde. Cells were infiltrated in 2.3 M sucrose and frozen in liquid nitrogen. Bound BCθ was monitored on ultrathin cryosections after immunolabeling with a rabbit polyclonal anti-biotin antibody and 10 nm protein-A gold (25). After BCθ binding, raft membranes were collected from floating low-density fractions (FLDF), rinsed, and sedimented at 200,000 $\times$ *g*, and the pellets then resuspended in PBS. FLDF were adsorbed to grids, fixed in 1% glutaraldehyde in PBS, and immunolabeled with anti-biotin and 10 nm protein-A gold. Alternatively, low-density membrane rafts were first isolated from washed platelets, adsorbed to grids, and incubated with BCθ at 4°C followed by fixation and immunolabeling as described (26). Sections and raft membranes were analyzed in a JEOL 1200CX electron microscope.

Fluorescence Labeling. Human A431 cells cultured in DMEM containing 10% FBS were incubated in a serum-free medium for 2 h to eliminate the effects of serum cholesterol. The cells were incubated with or without 5 mM 2OHpβCD at 37°C for 15 min.

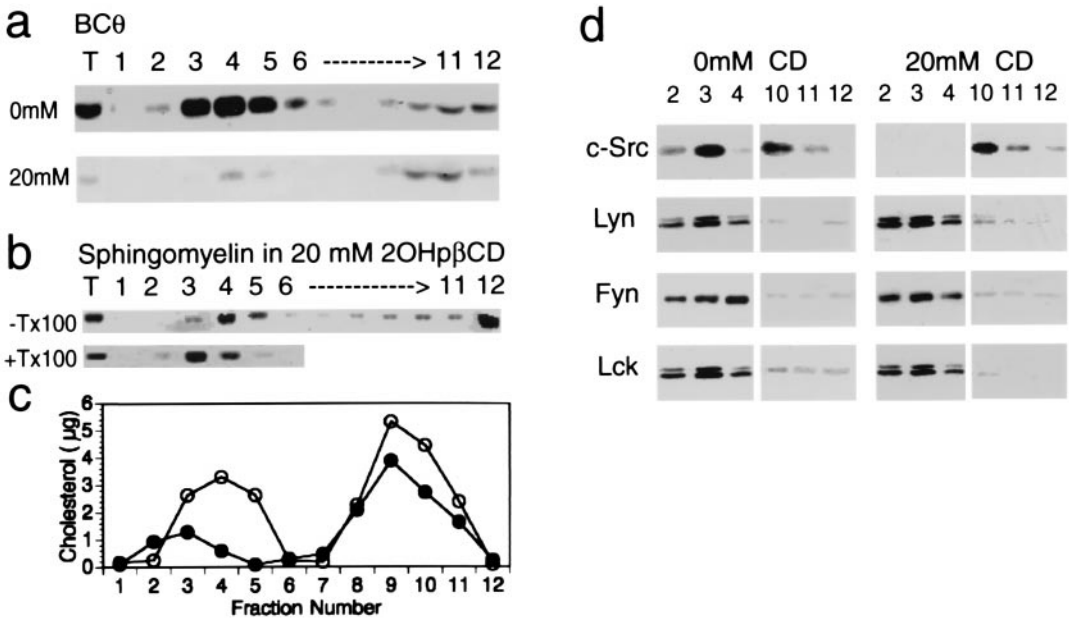

Fig. 4. Cholesterol depletion with 2OHpβCD completely reduces BCθ binding to FLDF. Platelets were incubated with 20 mM 2OHpβCD or buffer alone, followed by incubation with BCθ. Cell homogenates were fractionated into a sucrose gradient and analyzed as in Fig. 2. (*a*) BCθ binding to cholesterol-depleted (20 mM) and control (0 mM) platelets (Tx-treated). (*b*) Sphingomyelin distribution in cholesterol-depleted platelets treated with (+Tx) or without Tx (-Tx). (*c*) Cholesterol distribution in 2OHpβCD-treated (closed circles) or untreated (open circles) samples (+Tx). (*d*) The distribution of tyrosine-kinases in FLDF and bottom fractions (+Tx) of 2OHpβCD-treated (20mM CD) and untreated (0mM CD) platelets. T, total platelets. Distribution of sphingomyelin and membrane proteins was determined in platelets that were not incubated with BCθ as detailed in Fig. 2's legend.

The later steps were performed at room temperature. After washing with PBS, the cells were fixed in 4% formaldehyde for 30 min, extensively washed, and incubated either with BCθ (10 μg/ml in PBS/BSA) or filipin (65 μg/ml in PBS/BSA) for 30 min. After washing with PBS, the BCθ-treated cells were incubated with cy3-avidin (1 μg/ml in PBS/BSA) for 30 min. The cells were then washed with PBS, and fluorescence was detected with a Zeiss Axiophoto microscope. Incubation of fixed cells with cy3-avidin alone without BCθ treatment did not show labeling.

Results and Discussion

To check whether BCθ binding depends on the cholesterol content of intact cell membranes we depleted cholesterol from platelets with cyclodextrins and then performed the BCθ binding experiments. Our flow cytometric data (Fig. 1*a*) indicate that BCθ binds only to cholesterol-rich membranes. Cholesterol depletion by one third, which corresponds to a decrease from 33 to 24 mol% of cholesterol in platelets, almost completely abolished BCθ binding. This indicates that there is a threshold concentration of membrane cholesterol for toxin binding in intact cells, which is consistent with our previous observations with liposomes (14, 20). Cholesterol depletion from erythrocytes also gave similar results (data not shown). As cholesterol is enriched in rafts, we assumed that BCθ might bind selectively to rafts and carried out further studies.

Membrane rafts are isolated as Tx-insoluble fractions at 4°C, partly extracted in Tx at 37°C and completely extracted in 60 mM octyl glucoside even at 4°C (4, 27, 28). Our results show that BCθ that had bound to different cell types was retained in Tx-insoluble fraction at 4°C, partly extracted at 37°C, and completely extracted in octyl glucoside (Fig. 1*b*). These results show that BCθ binds to membrane regions that fulfill the raft criteria of detergent solubilization, suggesting a preferential binding of BCθ to membrane rafts.

Using a sucrose density gradient, we next isolated the detergent-insoluble complexes that float at low density due to their high lipid content (2, 27). We used platelets for this study as they contain specific marker proteins in membrane rafts. In agreement with previous reports (21, 28, 29), tyrosine kinases such as c-Src, Fyn, Lck (Fig. 2*e*), and Lyn (not shown in the figure) are enriched in FLDF. Cholesterol is enriched (36% of total) in FLDF at the interface of 5–36% sucrose (Fig. 2*c*, fractions 3–5). Sphingomyelin is also enriched in FLDF (Fig. 2*b*), confirming the FLDF as rafts.

When BCθ-bound platelets were treated with Tx at 4°C and fractionated on a sucrose gradient, BCθ was predominantly distributed in FLDF at the interface of 5–36% sucrose (Fig. 2*a*, Tx-treated, fractions 3–5). Selective binding of BCθ to isolated membranes in FLDF was also demonstrated by IEM (Fig. 3 *c* and *e*). Although more than 60% of cholesterol is distributed in the bottom fractions (Fig. 2*c*, fractions 8–11), very little binding of BCθ to cholesterol is observed in these fractions, suggesting that BCθ binds to a selective population of cholesterol.

To exclude the possibility of potential detergent-induced artifacts, modification of rafts, and/or redistribution of BCθ during extraction (1), we also isolated rafts without detergent treatment. After incubation with BCθ, the platelets were sonicated vigorously and floated into a sucrose gradient. Again BCθ distribution is enriched in FLDF (Fig. 2*a*, -Tx, fractions 4–6). The FLDF obtained without Tx detergent extraction were also enriched in cholesterol and sphingomyelin (Fig. 2 *c* and *b*). To exclude the possibility that free BCθ was liberated by sonication or with time, as a result of equilibration, had contaminated the FLDF, we carried out sucrose gradient sedimentation with free BCθ placed at the bottom of the centrifuge tube. BCθ was detected only in bottom fractions and not in FLDF (data not shown). BCθ detected in fractions 10 and 11 (Fig. 2*a*) probably represents a toxin that is liberated because of extensive sonication. To analyze whether the Tx-insoluble material is exclusively enriched in FLDF, the pellet obtained after extraction with Tx

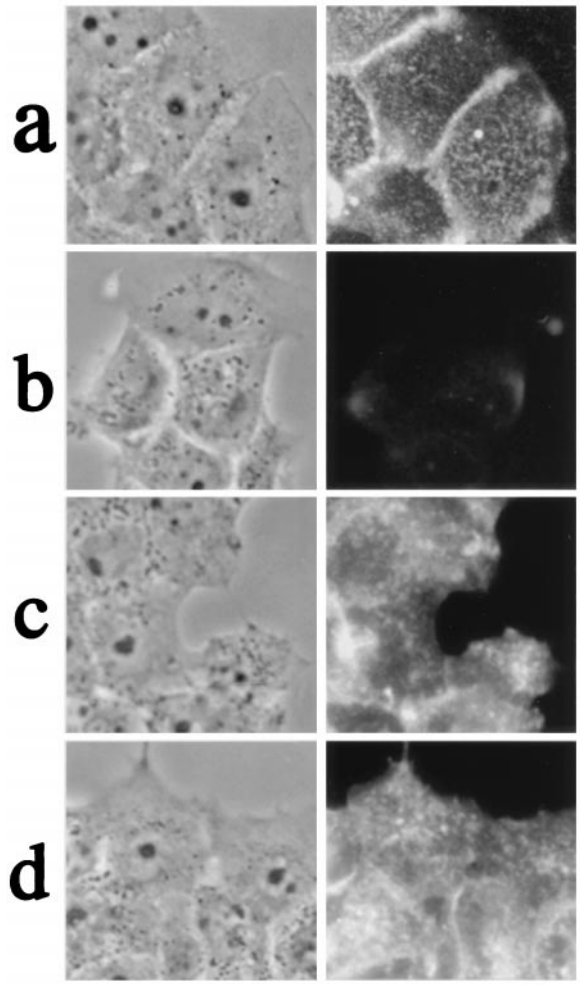

Fig. 5. Labeling of A431 cells with BCθ or filipin. Monolayer A431 cells were incubated with serum-free DMEM for 2 h, fixed, and then incubated with either BCθ or filipin. BCθ-treated cells were then incubated with cy3-avidin. (*a–d*) Binding of BCθ (*a* and *b*) or filipin (*c* and *d*) to 2OHpβCD-treated cells (*b* and *d*) or untreated controls (*a* and *c*). Depletion of cholesterol completely abolished BCθ binding, whereas filipin binding was retained significantly. (*Left*) Phase contrast; (*Right*) fluorescence staining.

at 4°C was mildly sonicated and fractionated on a sucrose gradient. Fig. 2*d* shows that more than 86% of cholesterol was distributed in FLDF (fractions 3–5), indicating that the Tx-insoluble material is enriched in FLDF in terms of cholesterol distribution. We therefore suggest that BCθ recovered in the Tx-insoluble fractions of erythrocytes, MOLT-4, and A431 cells (Fig. 1*b*) represents the portion bound to rafts. This is confirmed by our observations with erythrocytes, where BCθ distributed predominantly in FLDF (data not shown) when the isolated Tx-insoluble pellet of BCθ-bound erythrocytes (Fig. 1*b*, pellet at 4°C) was fractionated on the sucrose density gradient.

When cell surface cholesterol was monitored by immunoelectron microscopy (IEM), BCθ binding was readily detected on the cell surface of both erythrocytes and platelets (Fig. 3 *a* and *b*). In particular, on platelets the labeling was often preferentially concentrated in small cellular processes, suggesting formation of pseudopodia.

To analyze whether high cholesterol enrichment in rafts is required for BCθ binding, we depleted cholesterol from platelets and studied the profiles of BCθ binding. We used both MβCD and 2OHpβCD (30). They selectively encapsulate membrane cholesterol (30) and do not deplete lipids other than cholesterol at the concentrations used (data not shown). The light-scattering band that appears at the interface of 5–36% sucrose was considerably reduced after cholesterol depletion, probably because of disruption of the clustered raft-associated molecules (8, 9). A one-third cholesterol depletion obtained by treating platelets with 20 mM 2OHpβCD resulted in more than 90% reduction of BCθ binding (Fig. 4*a*, lane T). This was supported by our flow cytometric data (Fig. 1*a*). BCθ binding disappeared almost completely from FLDF after cholesterol depletion (Fig. 4*a*). Accordingly, the immunogold labeling was completely absent on isolated raft membranes (Fig. 3*d*). The cholesterol reduction was much more from FLDF (by 76%) than in bottom fractions (by 32%) (Fig. 4*c*), which is consistent with other reports (10). The higher depletion of cholesterol in FLDF would affect the mol % of cholesterol to greater extent, resulting in the complete disappearance of BCθ binding.

The distribution of c-Src in FLDF is also reduced (Fig. 4*d*), suggesting close association of this kinase with raft cholesterol directly or indirectly. On the other hand sphingomyelin and tyrosine kinases of Fyn, Lck, and Lyn are still enriched in cholesterol-depleted FLDF (Fig. 4 *b* and *d*). This suggests that some signaling molecules may be associated to form sphingolipid core-clusters without cholesterol (31). This is supported by our IEM observations showing high cholesterol content in only a subpopulation of the membranes floating at low density (Fig. 3*c*). Anti-CD36 antibodies bound to a majority of the isolated raft membranes (data not shown), indicating that most of the membranes obtained in FLDF are in the right-side-out position. The population of BCθ-unlabeled membranes therefore may represent the sphingomyelin-enriched plasma membrane microdomains and/or lipid-enriched raft membranes from intracellular origin. To test the latter we incubated isolated low-density membranes with BCθ after sucrose gradient fractionation, and monitored the binding of BCθ by IEM. Although more vesicles were labeled by BCθ in these preparations (Fig. 3*e*), a large population of membranes still remained devoid of label, suggesting that a heterogeneous population of membrane microdomains indeed exists.

Filipin has been used to study cholesterol distribution in membranes of fixed cells (32, 33). We used A431 cells to compare the labeling of BCθ to that of filipin. Although both the probes bind to cholesterol, filipin binds to membrane cholesterol indiscriminately—not only to plasma membranes, but also to intracellular membrane (Fig. 5*c*). On the other hand, BCθ binds only to plasma membrane cholesterol, because it does not permeabilize cells (Fig. 5*a*). Furthermore, in A431 cells the bound BCθ is retained in Triton-insoluble fractions (Fig. 1*b*), suggesting selective binding of BCθ to membrane microdomains. The reduction of cholesterol by 30% using 2OHpβCD completely abolished BCθ binding (Fig. 5*b*) while retaining significant filipin labeling (Fig. 5*d*). This difference in staining patterns clearly demonstrates distinct specificity of BCθ binding to cholesterol-rich membrane domains from indiscriminate binding of filipin to cell cholesterol. The critical reduction of cholesterol from the membrane microdomains as observed in platelets would be the cause for complete reduction of BCθ labeling in A431 cells on cholesterol depletion, because BCθ binds to cholesterol in cholesterol-rich artificial membranes (14, 20). These results further indicate the selectivity of BCθ binding to membrane microdomains of intact cells. Moreover, BCθ does not damage the cell membrane. On the other hand, filipin binding affects membrane integrity as it sequesters membrane cholesterol resulting in permeabilization of cells. Thus, BCθ is a powerful tool for detecting and monitoring rafts in living cells.

To determine whether binding of BCθ affects platelet function, we examined the platelet aggregation activity in the presence or absence of BCθ. BCθ caused neither platelet aggregation by itself, nor any significant change in the thrombin-induced

aggregation (data not shown). Fivaz *et al.* (5) proposed that toxins interacting with raft components would be interesting tools for studying rafts. BCθ binds preferentially to rafts without membrane damage. It therefore has much potential in elucidating not only the cholesterol integrity in rafts, but also the role of cholesterol in raft functioning. Selective binding of BCθ to a cholesterol-rich subpopulation of raft membranes (Fig. 3 *c* and *e*) can be used as a tool to isolate raft vesicles, and can help to identify the molecules present in these microdomains. Furthermore, because cholesterol depletion from platelets causes reduced BCθ binding (Fig. 1*a*) and impaired aggregation (unpublished results), binding of BCθ might be useful for monitoring the functional status of membrane rafts in these cells.

Rafts of plasma membranes have great functional significance in biological processes, including signal transduction, endocytosis, transcytosis, cholesterol transport, and bacterial and viral internalization (1–3, 28). Rafts are also involved in several diseases—such as prion diseases, Alzheimer's disease, and cancer (3, 34). The selectivity of BCθ for rafts may help elucidate the functional role of rafts in many cellular events and aid in understanding the function of these microdomains in health and disease. Because BCθ binds to living cells without membrane damage (11, 16), fluorescent-BCθ will also be a useful tool for monitoring raft dynamics in living cells. In this respect, monitoring cholesterol movement by single particle tracking experiments using BCθ would be promising.

We thank Dr. S. Suzuki for help with the coulter counter; Dr. H. Waki for TLC analysis; Dr. J. Shimizu for flow cytometric analysis; Dr. K. Aoki for technical advice; and Prof. Yoshitaka Nagai for support and encouragement. A.A.W. is a Science and Technology Agency fellow and Y.S. is a Domestic Research Fellow of Japan Science and Technology. This work was supported by grants from Japan Science and Technology, a Grant-in-Aid for Scientific Research of Japan Society for the Promotion of Science, and the Naito Foundation.

1. Hooper, N. M. (1998) *Curr. Biol.* **8,** 114–116.
2. Simons, K. & Ikonen, E. (1997) *Nature (London)* **387,** 569–572.
3. Brown, D. A. & London, E. (1998) *Annu. Rev. Cell Dev. Biol.* **14,** 111–136.
4. Brown, D. A. & London, E. (2000) *J. Biol. Chem.* **275,** 17221–17224.
5. Fivaz, M., Abrami, L. & van der Goot, F. G. (1999) *Trends Cell Biol.* **9,** 212–213.
6. Jacobson, K. & Dietrich, C. (1999) *Trends Cell Biol.* **9,** 87–91.
7. Varma, R. & Mayor, S. (1998) *Nature (London)* **394,** 798–801.
8. Friedrichson, T. & Kurzchalia, T. V. (1998) *Nature (London)* **394,** 802–805.
9. Hooper, N. M. (1999) *Mol. Membr. Biol.* **16,** 145–156.
10. Ostermeyer, A. G., Beckrich, B. T., Ivarson, K. A., Grove, K. E. & Brown, D. A. (1999) *J. Biol. Chem.* **274,** 34459–34466.
11. Iwamoto, M., Morita, I., Fukuda, M., Murota, S., Ando, S. & Ohno-Iwashita, Y. (1997) *Biochim. Biophys. Acta* **1327,** 222–230.
12. Ohno-Iwashita, Y., Iwamoto, M., Mitsui, K., Kawasaki, H. & Ando, S. (1986) *Biochemistry* **25,** 6048–6053.
13. Ohno-Iwashita, Y., Iwamoto, M., Mitsui, K., Ando, S. & Nagai, Y. (1988) *Eur. J. Biochem.* **176,** 95–101.
14. Ohno-Iwashita, Y., Iwamoto, M., Mitsui, K., Ando, S. & Iwashita, S. (1991) *J. Biochem.* **110,** 369–375.
15. Shimada, Y., Nakamura, M., Naito, Y., Nomura, K. & Ohno-Iwashita, Y. (1999) *J. Biol. Chem.* **274,** 18536–18542.
16. Fujimoto, T., Hayashi, M., Iwamoto, M. & Ohno-Iwashita, Y. (1997) *J. Histochem. Cytochem.* **45,** 1197–1205.
17. Hagiwara, H., Kogure, S., Nakamura, M., Shimada, Y., Ohno-Iwasita, Y. & Fujimoto, T. (1999) *Biochem. Biophys. Res. Commun.* **260,** 516–521.
18. Billington, S. J., Jost, B. H. & Songer, J. G. (2000) *FEMS Microbiol. Lett.* **182,** 197–205.
19. Rossjohn, J., Feil, S. C., McKinstry, W. J., Tweten, R. K. & Parker, M. W. (1997) *Cell* **89,** 685–692.
20. Ohno-Iwashita, Y., Iwamoto, M., Ando, S. & Iwashita, S. (1992) *Biochim. Biophys. Acta* **1109,** 81–90.
21. Dorahy, D. J., Lincz, L. F., Meldrum, C. J. & Burns, G. F. (1996) *Biochem. J.* **319,** 67–72.
22. Minowada, J., Ohunma, T. & Moore, G. E. (1972) *J. Natl. Cancer Inst.* **49,** 891–895.
23. Orlandi, P. A. & Fishman, P. H. (1998) *J. Cell Biol.* **141,** 905–915.
24. Amundson, D. M. & Zhou, M. (1999) *J. Biochem. Biophys. Methods* **38,** 43–52.
25. Heijnen, H. F. G., Debili, N., Vainchencker, W., Breton-Gorius, J., Geuze, H. J. & Sixma, J. J. (1998) *Blood* **91,** 2313–2325.
26. Liou, W., Geuze, H. J. & Slot, J. W. (1996) *Histochem. Cell Biol.* **106,** 41–58.
27. Brown, D. A. & Rose, J. K. (1992) *Cell* **68,** 533–544.
28. Rietveld, A. & Simons, K. (1998) *Biochim. Biophys. Acta* **1376,** 467–479.
29. Dorahy, D. J. & Burns, G. F. (1998) *Biochem. J.* **333,** 373–379.
30. Kilsdonk, E. P. C., Yancey, P. G., Stoudt, G. W., Bangerter, F. W., Johnson, W. J., Phillips, M. C. & Rothbalt, G. H. (1995) *J. Biol. Chem.* **270,** 17250–17256.
31. Ilangumaran, S. & Hoessli, D. C. (1998) *Biochem. J.* **335,** 433–440.
32. Kobayashi, T., Beuchat, M. H., Lindsay, M., Frias, S., Palmiter, R. D., Sakuraba, H., Parton, R. G. & Gruenberg, J. (1999) *Nat. Cell Biol.* **1,** 113–118.
33. Puri, V., Watanabe, R., Dominguez, M., Sun, X., Wheatley, C. L., Marks, D. L. & Pagano, R. E. (1999) *Nat. Cell Biol.* **1,** 386–388.
34. Anderson, R. G. W. (1998) *Annu. Rev. Biochem.* **67,** 199–225.